

Theme Issue Article

Vacuolisation of human microvascular endothelial cells by enterohaemorrhagic *Escherichia coli*

Martina Bielaszewska*¹; Andreas Bauwens*¹; Lilo Greune²; Björn Kemper³; Ulrich Dobrindt⁴; Joyce M. Geelen⁵; Kwang S. Kim⁶; M. Alexander Schmidt²; Helge Karch¹

¹Institute of Hygiene, University of Münster, Münster, Germany; ²Institute of Infectiology, Center for Molecular Biology of Inflammation (ZMBE), University of Münster, Münster, Germany; ³Center for Biomedical Optics and Photonics, University of Münster, Münster, Germany; ⁴Institute for Molecular Infection Biology, University of Würzburg, Würzburg, Germany; ⁵Department of Pediatric Nephrology, Radboud University Nijmegen Medical Centre, Nijmegen, The Netherlands; ⁶Division of Pediatric Infectious Diseases, Johns Hopkins University School of Medicine, Baltimore, Maryland, USA

Summary

Enterohaemorrhagic *Escherichia coli* (EHEC) cause haemolytic uraemic syndrome (HUS), a thrombotic microangiopathy resulting from endothelial injury in the renal glomeruli and other organs. EHEC virulence factors that damage the microvascular endothelium play therefore major roles in the pathogenesis of HUS. We identified an EHEC strain that vacuolates and kills primary human glomerular microvascular endothelial cells (GMVECs) and a human brain microvascular endothelial cell (HBMEC) line. Because the vacuolating effect closely resembles those elicited on other cells by the vacuolating cytotoxin of *Helicobacter pylori* (VacA), we designated the factor responsible for this effect EHEC vacuolating cytotoxin (EHEC-Vac). EHEC-Vac (a secreted non-serine protease protein) binds to HBMECs rapidly and irreversibly, vacuolates within 30 min after exposure and the effect is maximally apparent at 48 h. Despite the vacuoli-

sation, HBMECs survive for several days before they undergo necrosis. Electron and immunofluorescence microscopy demonstrate that the vacuoles induced by EHEC-Vac originate from lysosomes. Accordingly, they stain with neutral red indicating an acidic microenvironment. Similar to VacA, the EHEC-Vac-mediated vacuolisation is both prevented and reverted by the vacuolar proton pump inhibitor bafilomycin A1, suggesting a similar mechanism of vacuole formation by these toxins. Despite the similarity of phenotypes elicited by EHEC-Vac and VacA, genomic DNA from the EHEC-Vac-producing strain failed to hybridise to a *vacA* probe, as well as to probes derived from presently known *E. coli* vacuolating toxins. Through its microvascular endothelium-injuring potential combined with the ability to induce interleukin 6 release from these cells EHEC-Vac might contribute to the pathogenesis of HUS.

Keywords

Enterohaemorrhagic *E. coli*, haemolytic uraemic syndrome, vacuolating cytotoxin, EHEC-Vac, microvascular endothelial injury

Thromb Haemost 2009; 102: 1080–1092

Introduction

Enterohaemorrhagic *Escherichia coli* (EHEC) cause diarrhoea, bloody diarrhoea and haemolytic uraemic syndrome (HUS) worldwide (1, 2). HUS, a triad of thrombocytopenia, haemolytic anaemia and renal insufficiency, is the most common cause of

acute renal failure in children (3). Although precise mechanisms triggering haematologic and renal pathologies in HUS are incompletely understood, histopathological studies of patients who died of HUS demonstrate that the major lesion underlying HUS is thrombotic microangiopathy which mainly affects renal glomeruli, and results from microvascular endothelial injury (4,

Correspondence to:
Dr. Martina Bielaszewska
Institut für Hygiene
Universität Münster
Robert Koch Str. 41
48149 Münster, Germany
Tel.: +49 251 980 2849, Fax: +49 251 980 2868
E-mail: mbiela@uni-muenster.de

Financial support:
This study was supported by the Deutsche Forschungsgemeinschaft (DFG) program "Infections of the endothelium" SPP 1130 (grant no. KA 717/4–2), by a grant from the DFG-funded International Graduate School "Molecular interactions of pathogens with biotic and abiotic surfaces" (GRK 1409), by the DFG Collaborative Research Centers SFB293 (Project B5) and SFB479 (Project A1), by the ERA-NET PathoGenoMics (grants no. PTJ-BIO/0313937A and PTJ-BIO/0313937C), by the German Competence Network PathoGenoMik (PTJ-BIO/03U213BVBIIIIPG3), and by the German Federal Ministry for Education and Research (BMBF) research program "Biophotonics".

*Both authors contributed equally to this study.

Received: July 10, 2009
Accepted after major revision: October 6, 2009

Prepublished online: October 26, 2009
doi:10.1160/TH09-07-0499

5). The endothelial injury is thus the central event in the complex cascade that begins with gastrointestinal infection and culminates as renal insufficiency (2, 3).

Because of the key role of the microvascular endothelial damage in the pathogenesis of HUS, EHEC virulence factors that can injure human endothelium are likely to play a major role in the HUS development (6). EHEC, in contrast to other endothelium-injuring pathogens (7), do not enter the blood stream (2, 6). They presumably damage endothelial cells by elaborated molecules produced by EHEC colonising the gut, which have been translocated into the circulation and reach the target cells via systemic dissemination (1, 2, 6). The best studied EHEC endothelial injuring factors are Shiga toxins (Stxs) (8). These toxins bind to the target cells via their B subunit which recognises the glycosphingolipid globotriaosylceramide (Gb3Cer/CD77) receptor (9). After internalisation of the toxin via receptor-mediated endocytosis, the A subunit with *N*-glycosidase activity hydrolyses the 60S ribosomal subunit inhibiting protein synthesis, which leads to the cell death (8).

Recently, non-Stx EHEC proteins have been demonstrated to injure human microvascular endothelium, introducing them as candidate virulence factors involved in the pathogenesis of HUS. These molecules include cytolethal distending toxin (CDT)-V, a new member of the CDT family which is produced by EHEC O157 (10, 11) and particular non-O157 EHEC causing HUS (12), and a repeat-in-toxin (RTX) haemolysin designated EHEC haemolysin (13). The former is a genotoxin and cyclomodulin that causes DNA fragmentation in endothelial cells, triggers DNA-damage repair responses, arrests the cell cycle, and ultimately causes cell death (14). The latter is a pore-forming protein (15) that lyses human microvascular endothelial cells (16). Another EHEC molecule, subtilase cytotoxin (17) causes multi-organ microvascular thromboses in mice (17), which mimic lesions found in patients with HUS (4, 5); however, its toxicity towards the human endothelium remains to be demonstrated.

We screened our collection of EHEC clinical isolates for their ability to injure human endothelium, and identified a strain that strikingly vacuolated various endothelial cells. This effect closely resembled the effects of vacuolating cytotoxin (VacA) of *Helicobacter pylori* (18). Because such an effect is unusual in EHEC, we analysed the interaction of the EHEC vacuolating factor with human microvascular endothelial cells originating from organs that are critically affected during HUS (kidneys and brain) (4, 5) and characterised the vacuoles.

Materials and methods

Bacterial strains

Strain 6451/98 (serotype Orough:H45) was isolated from a patient with diarrhoea in Germany. The strain contains the *stx*_{2d} gene encoding non-activatable Stx_{2d}, but does not secrete detectable amounts of the toxin as demonstrated by the Vero cell assay and Stx immunoassays (19). Strain 6451/98 lacks other *stx* alleles and genes encoding other EHEC toxins including EHEC-*hlyA* encoding EHEC haemolysin (13), *subA/subB* operon encoding the subtilase cytotoxin (17), and *cdtI*, *cdtII*, *cdtIII*, *cdtIV*, and *cdtV* clusters encoding various CDTs (12). In addition, 60

EHEC strains belonging to serotypes O157:H7/NM (non-motile) (n = 15), O26:H11/NM (n = 15), O103:H2 (n = 9), O111:H8/NM (n = 10), and O145:H25/H28/NM (n = 11) which cause most HUS cases in Germany (1) were screened for their ability to cause vacuolisation of endothelial cells. The strains were isolated between 1996 and 2006 from patients with HUS (n = 50), bloody (n = 7) or non-bloody diarrhea (n = 3). Uropathogenic *E. coli* (UPEC) strains 536 (20) and CFT073 (21), laboratory strain *E. coli* XL1-Blue-MR (Stratagene, Heidelberg, Germany), and a clinical isolate of *H. pylori* were used as controls.

Preparation of cosmid library

Genomic DNA from strain 6451/98 was partially digested with *Sau3AI* (Gibco BRL, Eggenstein, Germany) and resulting fragments were dephosphorylated with shrimp alkaline phosphatase, ligated into the cosmid (SuperCos I; Stratagene) arms, and packaged into phage heads with the Gigapack III XL-4 system (Stratagene). *E. coli* XL1-Blue MR transductants were selected on Luria-Bertani (LB) agar containing ampicillin (100 µg/ml) and stored as a cosmid library. To screen the cosmid library for vacuolating effects towards human endothelial cells, the cosmids were grown overnight in LB broth containing ampicillin (100 µg/ml) and sterile supernatants were investigated on monolayers of human brain microvascular endothelial cells (HBMECs) as described below.

Cell cultures

The HBMEC line (22) was grown in RPMI 1640 (Lonza, Cologne, Germany) supplemented with 10% fetal calf serum (FCS) (PAA, Pasching, Austria), 10% Nu-Serum (Becton Dickinson Biosciences, Bedford, MA, USA), 2 mM L-glutamine, 1 mM sodium pyruvate, 1% non-essential amino acids, and 1% vitamin mix (Lonza) (14). For some assays, HBMECs were cultured in HEPES (4-(2-hydroxyethyl)-1-piperazineethanesulfonic acid)-buffered Leibowitz L-15 (PAA) supplemented with 10% FCS-Gold (PAA), 10% Nu-Serum, 1 mM sodium pyruvate, 2 mM L-glutamine, 1% non-essential amino acids, and 1% vitamin mix. Primary human glomerular microvascular endothelial cells (GMVECs) from kidneys of two different donors (not suitable for transplantation) were isolated, purified and cultured as described previously (23). They were used for experiments in passages 6 to 10.

Preparation of samples for cell culture assays

Strain 6451/98 was grown in LB broth overnight (37°C, 180 rpm), the culture was centrifuged (6.000 x g, 10 min, 4°C) and the supernatant was filtered through a 0.2 µm membrane filter (Corning Inc., Corning, N.Y., USA). The sterile supernatant was used in cell culture experiments immediately or after storage at -20°C for up to 2 months (freezing did not substantially reduce the vacuolating activity). To determine the influence of pH on the production of the vacuolating factor, LB broth with pH 7.0, 7.5, 8.0, and 8.5 was used for the culture. The effect of mitomycin C was assessed by growing the strain in LB broth, pH 7.0, without or with mitomycin C (0.5 µg/ml). Sterile culture supernatants prepared under different conditions were compared for their vacuolating titers on HBMECs.

Vacuolisation assay

HBMECs (3.5×10^4 cells/well) and GMVECs (1×10^4 cells/well) were grown in 24-well microtiter plates (Corning Inc.) overnight until ~60% confluence. The monolayers were exposed to two-fold dilutions of sterile supernatant of strain 6451/98 (800 μ l/well) and incubated (37°C, 5% CO₂) for 4 h or 24 h. Morphological changes were examined using a light microscope (Axiovert 100; Zeiss, Jena, Germany) and photographed (PowerShot A620; Zeiss). The vacuolating titer was defined as the highest dilution of the supernatant that caused vacuolisation in $\geq 50\%$ of the cells. This dilution was considered to contain a 50% vacuolating dose (VD₅₀). The dilution of supernatant 6451/98 which caused vacuolisation in $\geq 90\%$ of cells after 24 h was defined as a 90% vacuolating dose (VD₉₀). To determine the time course of the vacuolisation process, HBMEC monolayers were exposed to VD₉₀ of supernatant 6451/98 (dilution 1:4) for 30 min, 90 min, 4 h, 6 h, 18 h, 24 h, and 48 h (37°C, 5% CO₂). At each time interval, the amount and size of vacuoles in cells, and the proportion (%) of vacuolated cells in the monolayer were determined. For the latter purpose, cells in 10 randomly selected microscopic fields (altogether 100 – 160 cells) were counted and the percentage of cells containing >5 vacuoles was calculated. To investigate whether or not vacuolisation is reversible, HBMEC monolayers were exposed to VD₉₀ of supernatant 6451/98 for different time intervals (5 min, 15 min, 30 min, 1 h, 2 h, 3 h, 4 h, 6 h, and 24 h), the supernatant was then removed, cells were washed twice with medium and incubated in fresh medium up to 24 h. The proportion (%) of cells which developed vacuoles after each exposure time was determined as described above.

Neutral red staining

After incubation with VD₉₀ of supernatant 6451/98 for 4 h and 24 h, medium from the cell monolayers was removed and replaced with 500 μ l/well of 0.33% neutral red solution (Sigma-Aldrich, Taufkirchen, Germany) for 5 min at 37°C. After removing the dye, cells were examined microscopically as described above.

Effect of bafilomycin A1 on vacuolisation

The effect of bafilomycin A1 on vacuolisation was investigated using three different approaches (24–26). First, HBMEC monolayers in 24-well plates were pre-treated (45 min, 37°C) with 25 nM, 50 nM or 100 nM bafilomycin A1 (Sigma-Aldrich). A VD₉₀ of supernatant 6451/98 was then added, in parallel, to bafilomycin A1-treated cells and to control (untreated) cells and the extents of vacuolisation (determined as the percentage of vacuolated cells in the respective cultures using the approach described above) were compared after incubation for 24 h at 37°C. Second, bafilomycin A1 at the above concentrations was added to HBMECs simultaneously with VD₉₀ of supernatant 6451/98. After 24 h of incubation, the extent of vacuolisation of cells treated with each mixture of supernatant 6451/98 and bafilomycin A1 (25 nM, 50 nM, and 100 nM) was compared with that of cells treated with VD₉₀ of supernatant 6451/98 alone. Third, to determine the effect of bafilomycin A1 on preformed vacuoles, HBMEC monolayers in 24-well plate were pre-vacuolated by incubation with VD₉₀ of supernatant 6451/98 overnight. Bafilomycin A1 (25 nM, 50 nM or 100 nM) was then added to the

cell culture medium and the incubation was continued for 4 h and for 24 h. At each time interval, the extent of vacuolisation of the bafilomycin A1-treated cells was compared with that of control cells incubated in the absence of bafilomycin A1. In each experiment, HBMECs treated with each respective concentration of bafilomycin A1 and with the corresponding amount of dimethyl sulfoxide used to dissolve bafilomycin A1 were included as controls.

Transmission electron microscopy

Transmission electron microscopy was performed as described (27), with slight modifications. Briefly, after incubation for 24 h with VD₉₀ of supernatant 6451/98 HBMECs were fixed with 2% glutaraldehyde in Dulbecco's phosphate buffered saline (D-PBS), pH 7.4, for 24 h at 4°C, washed three times with D-PBS and postfixed with 1% osmium tetroxide. After three washes with D-PBS the samples were dehydrated by a graded ethanol series (30%, 50%, 70%, 90%, and 96% for 15 min each, twice 99% for 30 min) and embedded in epoxy resin at 60°C for 48 h. Ultra-thin sections were prepared and stained with uranyl acetate and Reynold's lead citrate and examined using a Fei Tecnai Spirit Twin electron microscope (FEI Deutschland GmbH, Frankfurt/Main, Germany).

Fluorescence microscopy

HBMECs were grown on 4-well Permanox Lab-Tek Chamber Slides (Nunc GmbH, Langenselbold, Germany) seeded with 5×10^4 cells/well until ~60% confluence. The monolayers were infected with VD₉₀ of supernatant 6451/98 and incubated for 24 h (37°C, 5% CO₂). The cells were washed twice with PBS (Lonza), fixed with 3.7% paraformaldehyde (30 min at room temperature) and permeabilised with 0.25% Triton-X100 in PBS (1 min at room temperature). After blocking with 5% bovine serum albumin (BSA) and 0.2% fish skin gelatine (Sigma-Aldrich) in PBS (2 h at room temperature), primary antibody (diluted 1:100 in PBS with 1% BSA) was added and slides were incubated overnight at 4°C. The primary antibodies against cell organelles (all Sigma-Aldrich, derived from rabbits) were anti-GM130 (Golgi complex), anti-protein disulfide isomerase (PDI) (endoplasmic reticulum), anti-lysosome-associated membrane protein 1 (LAMP1) (lysosomes), and anti-Rab 11 (recycling endosomes). After incubation with primary antibody, slides were washed three times and incubated with Alexa 488-conjugated goat anti-rabbit IgG (Molecular Probes, Karlsruhe, Germany) diluted 1:1000 in PBS with 1% BSA for 1 h at room temperature. After washing, slides were stained with DAPI (4',6-diamidino-2-phenylindol) (Sigma-Aldrich) diluted 1:1000 in PBS (10 min at room temperature), mounted in an antifade mounting medium (Dianova, Hamburg, Germany) and examined with a fluorescence microscope (Axio Imager.A1, Zeiss). To detect early and late endosomes, Cy5-labelled transferrin (Dianova) (75 μ g/ml) was added to the cells 3 min and 25 min, respectively, before the end of incubation with supernatant 6451/98; the slides were then washed, fixed, stained with DAPI and mounted as described above.

Cell viability and apoptosis detection

The viability of HBMECs incubated with VD₉₀ of supernatant 6451/98 for 7 days was monitored by staining with 0.2% trypan

Table 1: PCR primers used to create DNA probes for Southern blot hybridisation of strain 6451/98.

Primer ^a	Sequence (5' - 3')	Target (DNA probe)	GenBank acc. No	Position	PCR conditions ^b			Size of amplicon (bp)
					Denaturation	Annealing	Extension	
VATs VATas	TCCTGGGACATAATGGTCAG GTGTCAGAACGGAATTGT	<i>vat</i> (<i>vat</i>)	AY151282	1076–1095 2056–2038	94°C, 30 s	54°C, 60 s	72°C, 60 s	981
Sat 4 Sat 5	TATCAATGTATGGGCGAGAG AGCCAGCACGAAAACCTATGA	<i>sat</i> (<i>sat-4</i>)	AF289092	161–181 598–578	94°C, 30 s	52°C, 60 s	72°C, 60 s	438
Sat 6 Sat 7	GGCAGAGACCAACCCTACAAC TACCACCGTACCAAATCCA	<i>sat</i> (<i>sat-6</i>)	AF289092	501–521 1096–1076	94°C, 30 s	52°C, 60 s	72°C, 60 s	596
Sat 8 Sat 9	AGTGGTGAACGAAGTCTGTG TACGACCGTCTTTTTCACCTT	<i>sat</i> (<i>sat-8</i>)	AF289092	3274–3294 3757–3737	94°C, 30 s	56°C, 60 s	72°C, 60 s	484
VacA-1 VacA-2	TTTTTAGGAACGCTTTGGTG ATTCCCCACCCATCATCACT	<i>vacA</i> (<i>vacA</i>)	AE000598	3449–3468 3763–3744	94°C, 30 s	52°C, 60 s	72°C, 60 s	315

^aPrimer pair VATs/VATas was described previously (34). The other primers were designed in this study. ^bAll PCRs included 30 cycles as specified in the table preceded by initial denaturation (94°C, 5 min) and followed by final extension (72°C, 5 min).

blue (Sigma-Aldrich). The metabolic activity of the cells was determined daily using the WST-1 assay (Roche, Mannheim, Germany) which exploits the mitochondrial reduction of the tetrazolium salt WST-1 to formazan. The assay was performed in 96-well plates seeded with 6×10^2 /well of HBMECs (14) and absorbance was measured at 450 nm and reference wavelength 650 nm using an ELISA reader (Emax precision microplate reader, MWG Biotech, Ebersberg, Germany). Cells that were untreated or treated with 300 nM nocodazole (Sigma-Aldrich), respectively, served as controls. Apoptosis was measured by flow cytometric determination (FACScalibur; Becton Dickinson, Heidelberg, Germany) of the proportion of hypodiploid nuclei using the method of Nicoletti et al. (28) as described earlier (14). The net apoptosis elicited by EHEC-Vac was calculated as the difference between the percentage of apoptotic cells induced by EHEC-Vac and that induced by LB broth. Staurosporine (1 μ M) served as a positive control.

Digital holographic microscopy

To gain a closer insight into the destiny of vacuolated cells, we applied a minimally invasive single cell analysis approach using quantitative phase contrast imaging by digital holographic microscopy (DHM). For this purpose, an inverse microscope (iMIC, Till Photonics, Gräfelfing, Germany) with attached DHM module (engineered at the Center for Biomedical Optics and Photonics, University of Münster, Münster, Germany) (29) and equipped with an incubator for stabilised temperature (Solent Scientific Ltd., Segensworth, United Kingdom) was applied. HBMECs grown in HEPES-buffered Leibowitz L-15 medium in μ -dishes (ibidi GmbH, Munich, Germany) were vacuolated by exposure to VD₉₀ of supernatant 6451/98 for 22 h. Digital holograms of single vacuolated cells were then recorded continuously up to 72 h when all observed cells were dead. The coherent light source for the recording of digital holograms was a frequency doubled Nd:YAG laser (Compass 315M-100, Coherent, Lübeck, Germany, $\lambda = 532$ nm). In addition to the DHM time-lapse analysis, representative images of the cells under white light illumination were captured. The numerical reconstruction of the

digitally captured holograms was performed by non-diffractive reconstruction (30) with software developed at the Center for Biomedical Optics and Photonics (Münster, Germany). The resulting quantitative phase contrast images were used to monitor the cells' shape (30) and refractive index alteration of vacuoles.

Examination of inflammatory response

To investigate the ability of EHEC-Vac to elicit an inflammatory response from HBMECs, the cells were incubated with VD₉₀ of supernatant 6451/98 for 24 h and 4 days. The concentrations of interleukin (IL)-6 and IL-8 in cell culture supernatants were determined using commercially available enzyme-linked immunosorbent assay (ELISA) kits (RayBiotech, Inc., Norcross, GA, USA) (sensitivities of <3 pg/ml and <1 pg/ml, respectively) according to the manufacturer's instructions. To calculate net IL-6 and IL-8 responses to VD₉₀ of EHEC-Vac, the response elicited by a 1:4 dilution of LB broth in each assay was subtracted from that caused by the 1:4 dilution of supernatant 6451/98 containing VD₉₀ of EHEC-Vac. The cytokine release induced by VD₉₀ of supernatant 6451/98 was compared with that induced by supernatant of *E. coli* XL1-Blue MR.

The nature of the vacuolating factor

Aliquots of two-fold dilutions of supernatant 6451/98 (1:2 to 1:64) were heated to 56°C or 70°C for 30 min, to 99°C for 10 min, or treated with proteinase K (Sigma-Aldrich) (final concentration 50 μ g/ml) for 10 min and 30 min at 37°C. Vacuolating titers of the treated preparations were compared with that of untreated supernatant using HBMEC monolayers. To investigate influence of the serine protease inhibitor phenylmethylsulfonyl fluoride (PMSF) on the activity of the vacuolating factor, two-fold dilutions of supernatant 6451/98 were pre-incubated with 1 mM or 10 mM PMSF for 30 min at 37°C and vacuolating titers on HBMECs were compared with that of PMSF-untreated supernatant after 24 h of incubation. Cells incubated for 24 h with 1 mM and 10 mM PMSF alone served as controls to exclude a non-specific vacuolisation caused by PMSF.

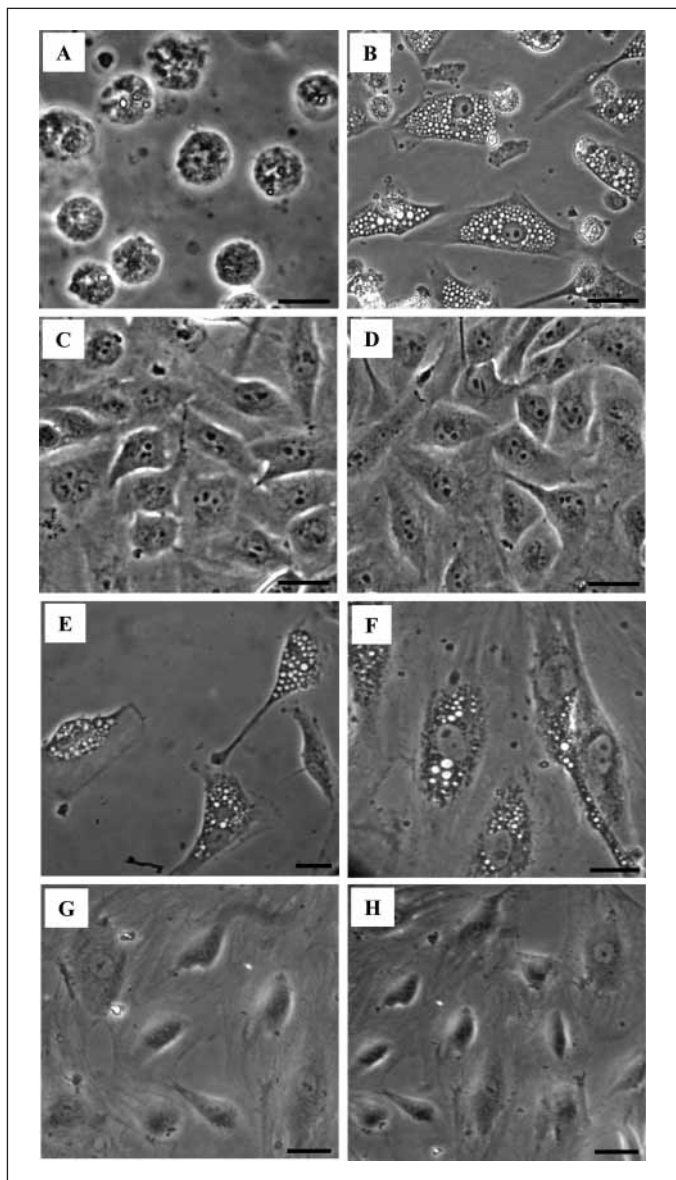


Figure 1: Morphological effects of supernatant of strain 6451/98 containing EHEC vacuolating cytotoxin (EHEC-Vac) on human microvascular endothelial cells. A-D) HBMECs incubated with supernatant 6451/98 for 4 h (dilution 1:2) (A), and for 24 h (dilution 1:4 containing VD_{90}) (B), and with LB broth for 24 h (C); D) control untreated cells after 24 h. E-H) Primary human glomerular microvascular endothelial cells (GMVECs) from donor #86 (E) and #76 (F) incubated for 24 h with supernatant 6451/98 (dilution 1:2), and with LB broth (donor #86) (G); H) control (untreated) cells from donor #86 after 24 h. Bars in panels A-D are 20 μ m and in panels E-H 50 μ m. Photomicrographs shown are representatives of six (HBMECs) and three (GMVECs) independent experiments.

Southern blot hybridisation, PCR and nucleotide sequencing

Genomic DNA from strain 6451/98 was digested (*Bam*HI and *Pst*I; New England Biolabs, Frankfurt, Germany), separated in 0.6% agarose, and transferred to a nylon membrane (Roti[®]-Nylon plus, Carl Roth GmbH, Karlsruhe, Germany). Immobilised separated DNA fragments were probed under stringent con-

ditions with digoxigenin-labeled probes (Table 1) derived from published sequences of *VacA* of *H. pylori* (GenBank accession number AE000598) (31) and of *E. coli* autotransporters with known vacuolating activity towards mammalian cells including vacuolating autotransporter toxin (*Vat*) of avian pathogenic *E. coli* strain Ec222 (GenBank accession number AY151282) (32) and secreted autotransporter toxin (*Sat*) of UPEC strain CFT073 (GenBank accession number AF289092) (33). Hybridisation was achieved with the DIG DNA Labelling and Detection Kit (Roche Molecular Biochemicals, Mannheim, Germany).

PCR was performed as described (11) using primers in Table 1. The amplicons were sequenced using an automated ABI Prism 3130xl Genetic Analyser and the ABI Prism BigDye Terminator Ready Reaction Cycle Sequencing Kit (version 3.1, Applied Biosystems, Darmstadt, Germany). Sequences were analysed using the Ridom TraceEditPro Software (Ridom GmbH, Würzburg, Germany) and homology was sought on the EMBL-GenBank database (<http://www.ncbi.nlm.nih.gov/BLAST>).

Screening of EHEC for vacuolating activity

Sterile culture supernatants of 60 EHEC strains grown in LB broth (18 h, 37°C, 180 rpm) were diluted 1:4 with cell culture medium and investigated using the vacuolisation assay on HBMECs immediately after preparation.

Statistical analysis

The statistical analysis of results was performed using Student's *t*-test; $p \leq 0.05$ was considered significant.

Results

Effects of strain 6451/98 on human microvascular endothelial cells

Upon exposure of HBMEC monolayers to serially diluted sterile supernatant of strain 6451/98 different effects were observed. A 1:2 dilution of the supernatant killed HBMECs within 4 h, as manifest by rounding cells and the inability to exclude trypan blue (Fig. 1A); after 24 h most of the cells were detached from the plastic support. This effect was not caused by Stx, because the sole *stx* gene in this isolate, *stx*_{2b} is not expressed (19). At a dilution of 1:4, multiple vacuoles were visible in $\geq 90\%$ of the cells after 24 h (VD_{90}) (Fig. 1B). At the same time point, the amounts of cells in monolayers treated with VD_{90} of supernatant 6451/98 (Fig. 1B) were $\sim 50\%$ of those present in control untreated monolayers (Fig. 1D), indicating persisting cytotoxicity. The titer of the vacuolating activity in supernatant 6451/98 was 1:16. It was independent of pH of the LB culture medium (7.0, 7.5, 8.0, or 8.5) and presence of mitomycin C during culture (data not shown). No cytotoxicity or vacuolisation were observed in cells exposed for 24 h to LB broth (used to prepare the supernatant of strain 6451/98) (Fig. 1C) and in control (untreated) cells (Fig. 1D). This indicates that the cytotoxic and vacuolating effects were specifically mediated by a factor secreted by strain 6451/98.

Supernatant of strain 6451/98 also extensively vacuolated GMVECs, derived from kidneys, which are the direct targets affected during HUS (4). After 24 h of exposure to a 1:2 dilution of the supernatant, $\geq 90\%$ cells were heavily vacuolated (Fig. 1E

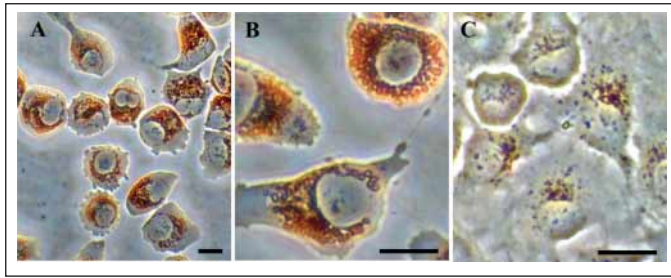


Figure 2: Neutral red staining of vacuoles induced by EHEC-Vac on HBMECs. A) Cells were treated with VD_{90} of EHEC-Vac for 24 h and then stained with neutral red (5 min, $37^{\circ}C$). B) A higher magnification of the neutral red-stained cells. C) Control untreated cells stained with neutral red. Bars indicate 20 μm . Photomicrographs shown are representatives of seven independent experiments.

and F). Moreover, similar to HBMECs, the total cell numbers in GMVEC cultures treated with supernatant 6451/98 (Fig. 1E and F) were $\leq 50\%$ of those in cultures exposed to LB broth (Fig. 1G) and in untreated cultures (Fig. 1H) demonstrating the cytotoxicity of supernatant 6451/98 towards GMVECs. The vacuolating titers on cells originating from two different donors were 1:8 and 1:4, respectively. The effects of supernatant 6451/98 on the morphologies of HBMECs and GMVECs resembled those produced by VacA on several non-endothelial cell lines (18). Based on its striking vacuolating capacity and cytotoxicity to endothelial cells we designated the putative secreted molecule of strain 6451/98 involved in these changes as “EHEC vacuolating cytotoxin” (EHEC-Vac).

Neutral red staining

Neutral red staining of HBMECs exposed to VD_{90} of EHEC-Vac for 4 h and 24 h demonstrated that at each time interval, the ma-

jority of vacuoles accumulated a visible amount of the dye (Fig. 2A and B). The same was true for vacuoles in GMVECs which were analysed after 24 h (data not shown). This indicates that similar to vacuoles induced by VacA of *H. pylori* which uniformly stain with neutral red because of their acidic content (35), the microenvironment in the vacuoles induced by EHEC-Vac in the endothelial cells is acidic.

Time course of vacuolisation caused by EHEC-Vac

To determine the kinetics of the vacuolating process, HBMECs were exposed to VD_{90} of EHEC-Vac for intervals ranging from 0.5 to 48 h (Fig. 3). At each time, the proportion of vacuolated cells in the monolayer and the amount and size of vacuoles in the cells were measured. The first vacuolisation, manifest as scarce tiny vacuoles in $\sim 20\%$ of cells, was visible after 30 min. By 90 min, $\sim 50\%$ of cells contained vacuoles which increased in the number per cell (~ 100), but remained small in diameter. By extending the time of exposure, the size of the vacuoles and the proportion of vacuolated cells in the monolayers increased (Fig. 3). After 18 h, $\sim 90\%$ of cells contained mostly mid-sized and large vacuoles. These vacuoles frequently fused (Fig. 3, panels 18 h and 24 h) suggesting that the huge vacuoles observed after 24 h and 48 h might have arisen by fusion of smaller vacuoles; this is supported by a decreasing number of vacuoles in parallel with their increasing size (Fig. 3, panels 24 h and 48 h). The large vacuoles filled most of the cytoplasm and dislocated the nucleus to the cell periphery (Fig. 3, panels 24 h and 48 h). The extent of vacuolisation did not substantially increase beyond 48 h (data not shown).

EHEC-Vac binds to HBMECs rapidly and irreversibly

To assess the minimum exposure time necessary for EHEC-Vac to trigger vacuolisation of HBMECs, and to determine if the vacuolating effect is reversible by depleting the toxin, the cells were

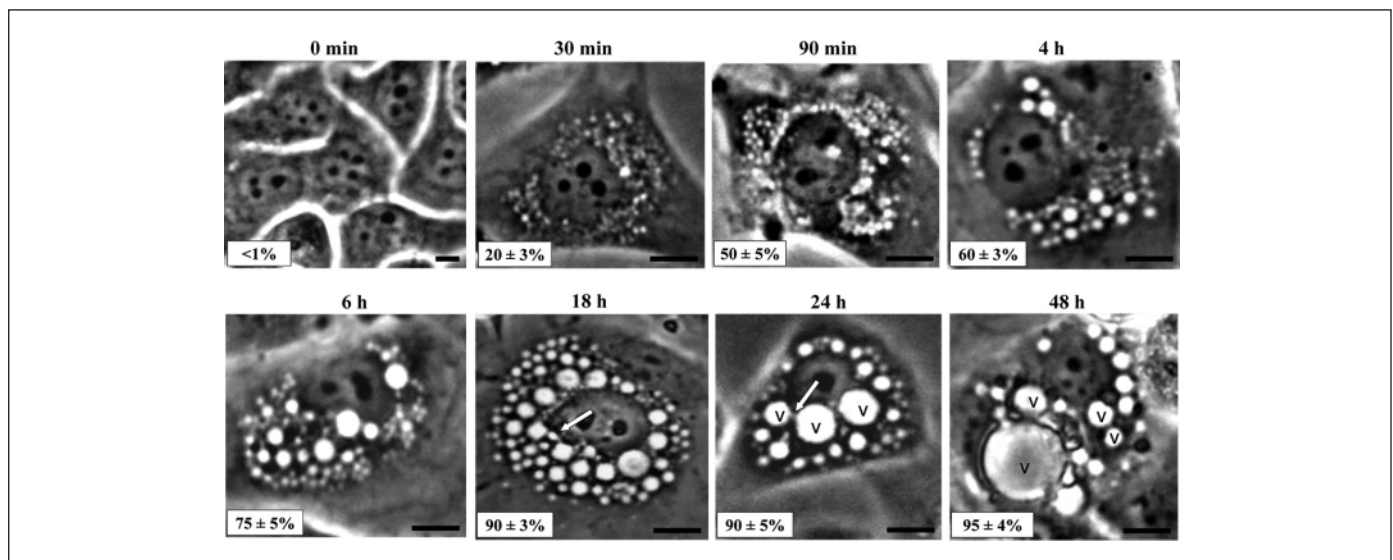


Figure 3: Time course of vacuolisation induced by EHEC-Vac on HBMECs. Cells were exposed to VD_{90} of EHEC-Vac for indicated time intervals and at each time point, the proportion of vacuolated cells in the culture and the amount and size of vacuoles in cells were determined. Time 0, control (untreated) cells. In panels 30 min to 48 h, the vacuolating phenotypes typical for the respective time points and the percentage of vacuolated cells in the cultures (expressed as means \pm SD from three independent experiments) are shown. In each time interval, between 100 and 160 cells were analysed to determine the percentage of vacuolated cells. Arrows in panels 18 h and 24 h depict fusing vacuoles (v). Bars indicate 10 μm .

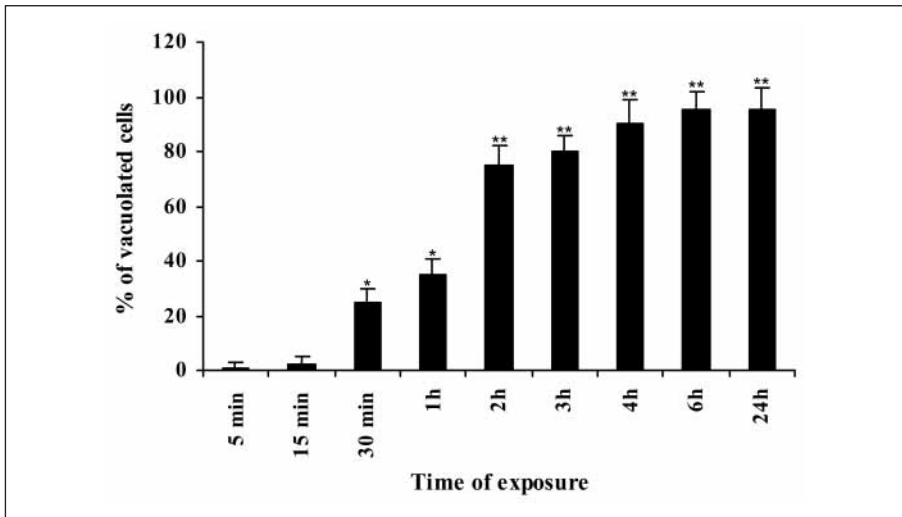


Figure 4: EHEC-Vac binds to HBMECs rapidly and irreversibly. HBMEC monolayers were incubated with VD_{90} of EHEC-Vac for the indicated times. The toxin was then removed, cells were washed with medium and incubated in fresh medium up to 24 h. After each time of exposure, the percentage of vacuolated cells in monolayers was determined. Data shown are means \pm standard deviations of three independent experiments. * $p < 0.01$, and ** $p < 0.001$ as compared to 5 min exposure time (unpaired Student's t-test).

exposed to VD_{90} of EHEC-Vac for various time intervals (5 min to 24 h) (Fig. 4). After each exposure, the toxin was removed, cells were washed and incubated in fresh medium up to 24 h when the proportions of vacuolated cells in monolayers were determined. A significant vacuolisation affecting ~25% of cells was triggered by exposure as brief as 30 min ($p < 0.01$ as compared to the exposure of 5 min) (Fig. 4). With increasing exposure time, the proportion of vacuolated cells in monolayers steadily increased and plateaued after 4-h exposure when 90% of cells were vacuolated (Fig. 4). This suggests that EHEC-Vac binds to HBMECs rapidly and irreversibly.

Effect of bafilomycin A1 on vacuolisation mediated by EHEC-Vac

Bafilomycin A1, a specific inhibitor of vacuolar-type H^+ -ATPases (36), inhibits the formation of vacuoles in response to *H. pylori* VacA (24, 37). It also reverts vacuolisation elicited by this toxin, leading to disappearance of vacuoles from vacuolated cells (37). Pre-incubation of HBMECs for 45 min with various bafilomycin A1 concentrations (25 nM, 50 nM and 100 nM) completely prevented vacuolisation caused by VD_{90} of EHEC-Vac after 24 h (Fig. 5A and B). Moreover, each of the bafilomycin A1 concentrations completely inhibited formation of vacuoles by VD_{90} of EHEC-Vac when the toxin and bafilomycin A1 were added to HBMEC simultaneously for 24 h (Fig. 5C and D). Finally, 100 nM and 50 nM bafilomycin A1 added for 4 h to HBMECs pre-vacuolated with VD_{90} of EHEC-Vac significantly reduced the extent of vacuolisation (from $> 90\%$ to $30 \pm 5\%$ and $50 \pm 4\%$, respectively; $p < 0.001$) (Fig. 5E and F); 25 nM bafilomycin A1 minimally affected pre-vacuolated cells after 4 h of contact. However, each of the bafilomycin A1 concentrations completely reverted vacuolisation caused by VD_{90} of EHEC-Vac after 24 h of contact with pre-vacuolated HBMECs, and restored normal cellular appearance (Fig. 5G and H). The fact that vacuolisation induced by EHEC-Vac is, similar to that caused by VacA, both inhibited and reverted by bafilomycin A1, suggests that the mechanism of vacuole formation induced by EHEC-Vac might be the same as, or similar to, that reported for VacA (38, 39).

Origin of vacuoles induced by EHEC-Vac

To determine the origin of vacuoles induced by EHEC-Vac, we analysed HBMECs by transmission electron microscopy. This demonstrated multiple electron lucent, membrane-surrounded cytoplasmic vacuoles in cells exposed for 24 h to VD_{90} of EHEC-Vac (Fig. 6B); these vacuoles were absent from untreated cells (Fig. 6A). Most of the vacuoles contained heteromorphic lamellar and vesicular structures (Fig. 6C). Such structures are typical components of lysosomes and represent material accumulated in the lysosomes for subsequent enzymatic digestion (40). The other cell organelles including nucleus, mitochondria, Golgi complex, endoplasmic reticulum, and early and late endosomes were well preserved, showing no obvious alterations (Fig. 6C). This suggests that EHEC-Vac acts selectively on lysosomes and that the vacuoles elicited by the toxin may be derived from these organelles.

Immunofluorescence staining of HBMECs exposed to EHEC-Vac for 24 h using markers for different cellular compartments involved in membrane trafficking demonstrated that endosomes (early, late, recycling), endoplasmic reticulum and Golgi complex in such cells had the same subcellular distribution as in control (untreated) cells (data not shown). No staining of vacuoles was observed using the respective organelle markers (data not shown) indicating that the vacuoles did not contain components of these organelles. In contrast, anti-LAMP1 antibody, which is specific for the lysosomal membrane, associated with the vacuolar membranes and bound to multiple EHEC-Vac-induced cytoplasmic vacuoles (Fig. 7B, D, and F); lysosomes in control (untreated) cells showed normal distribution (Fig. 7H). These data corroborate the electron microscopic observation that the vacuoles are most likely derived from lysosomes.

Mechanism of death of vacuolated cells

To determine viability of vacuolated HBMECs, we monitored the metabolic activity of cells exposed to VD_{90} of EHEC-Vac for 7 days using the WST-1 assay. In contrast to control (untreated) cells, which displayed almost a linear increase in their metabolism, the metabolic activity of EHEC-Vac-treated cells was significantly reduced at day 2 after exposure and remained nearly

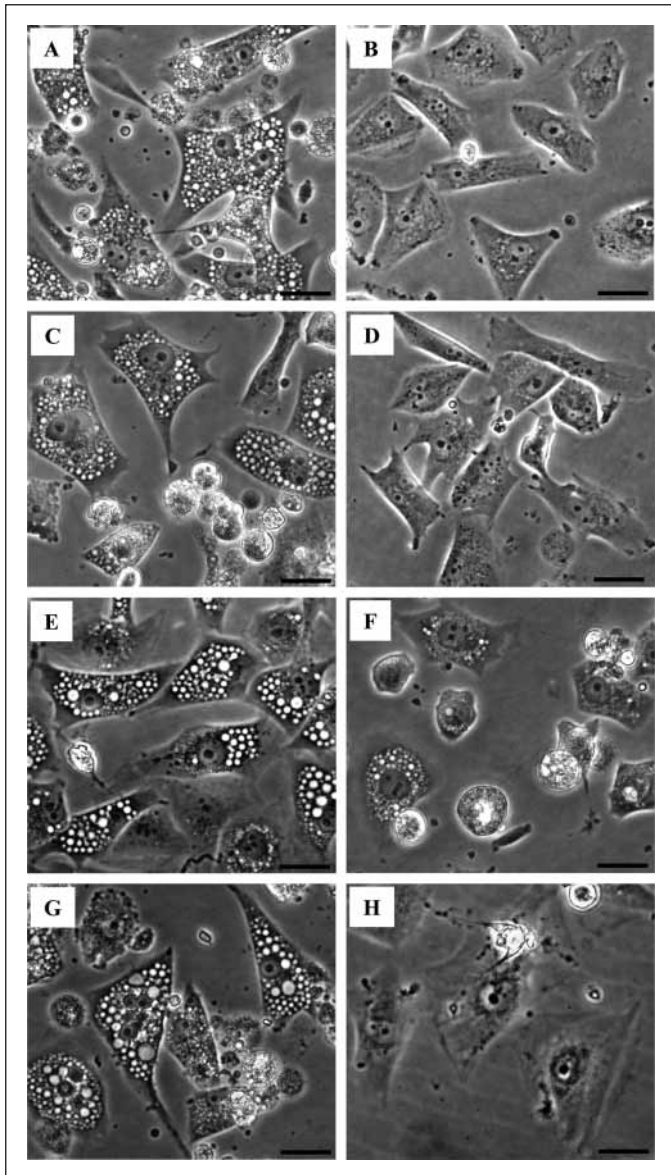


Figure 5: Bafilomycin A1 inhibits and reverts vacuolisation caused by EHEC-Vac. A and B) HBMEC monolayers were pre-treated with 25 nM bafilomycin A1 for 45 min (B) or left untreated (A) and then exposed to VD_{90} of EHEC-Vac for 24 h. C and D) VD_{90} of EHEC-Vac was added to HBMEC monolayers either alone (C) or simultaneously with 50 nM bafilomycin A1 (D) and cells were incubated for 24 h. E-H) HBMECs were pre-vacuolated by overnight incubation with VD_{90} of EHEC-Vac; bafilomycin A1 (100 nM) was then added to the cells for 4 h (F) and for 24 h (H). E and G), control cells treated with EHEC-Vac overnight and incubated for additional 4 h (E) and 24 h (G) without bafilomycin A1. Bars are 20 μ m. The photomicrographs shown are representatives of three independent experiments performed under each of the different conditions described.

constant with a slight decrease on day 7 (Fig. 8). These results agree with the reduced cellular density observed in HBMEC monolayers exposed to VD_{90} of EHEC-Vac for 24 h (Fig. 1) and confirm its toxicity towards HBMECs.

To identify the mechanism of the cell death, we analysed HBMECs exposed to VD_{90} of EHEC-Vac for apoptosis and ne-

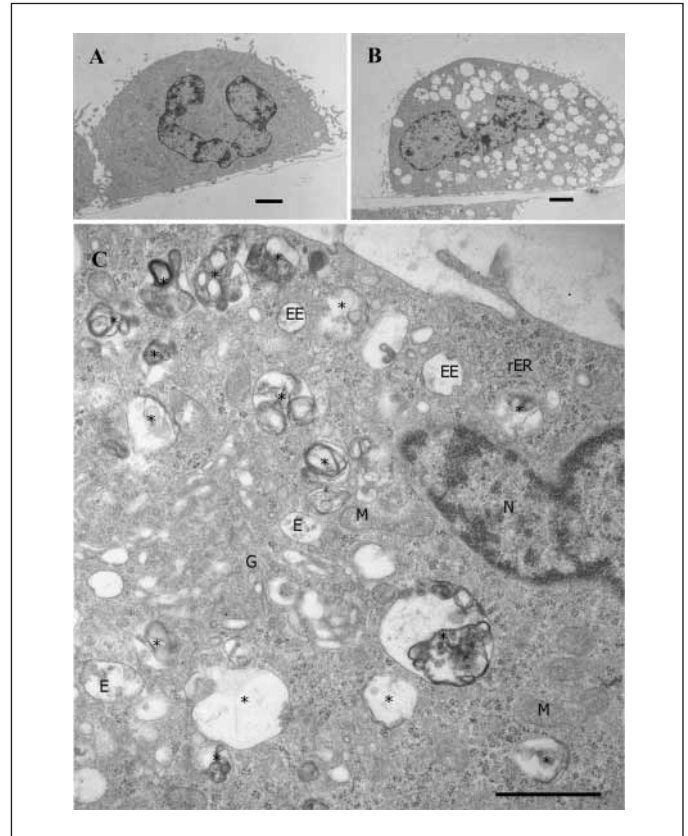


Figure 6: Transmission electron microscopy of HBMECs treated with EHEC-Vac. A) A control untreated cell after 24 h in culture medium. B) A cell exposed for 24 h to VD_{90} of EHEC-Vac. C) A detailed view of the cytoplasm of a vacuolated cell treated for 24 h with VD_{90} of EHEC-Vac. M, mitochondria; G, Golgi complex; E, endosome; EE, early endosome; N, nucleus; rER, rough endoplasmic reticulum. The asterisks depict the vacuoles (swollen lysosomes). Scale bars in panels A and B are 2 μ m and in panel C 1 μ m. Representative photomicrographs from one of at least 10 analysed cells are shown.

crois. The net proportion of cells with hypodiploid nuclei in monolayers exposed to EHEC-Vac for 7 days was $12 \pm 4\%$ (mean \pm standard deviation) as compared to $9 \pm 5\%$ ($p > 0.1$) and $45 \pm 10\%$ ($p < 0.01$) of such cells in control (untreated) monolayers and monolayers exposed to 1 μ M staurosporin, respectively. This demonstrated that the EHEC-Vac-treated cells did not undergo apoptosis.

To investigate if the EHEC-Vac-exposed HBMECs die via necrosis, we applied a single cell analysis using white light and quantitative DHM phase contrast imaging. Figure 9 demonstrates typical stages in the destiny of vacuolated cells. The cell "a" which was fully vacuolated after 21.8 h of exposure to VD_{90} of EHEC-Vac (Fig. 9A and B) rounded-up during the next 24.5 h ($t = 46.3$ h after exposure) (Fig. 9C), which led to a significant increase in the DHM phase contrast (Fig. 9D). After additional 25.4 h ($t = 71.7$ h) the cell poured out as shown in the white light image (Fig. 9E) and evidenced by the decrease of the cell's DHM phase contrast (Fig. 9F). A similar turn-over from fully vacuolated status to necrosis was observed for another cell (cell "b", Fig. 9C and D, and E and F, respectively), during an even short-

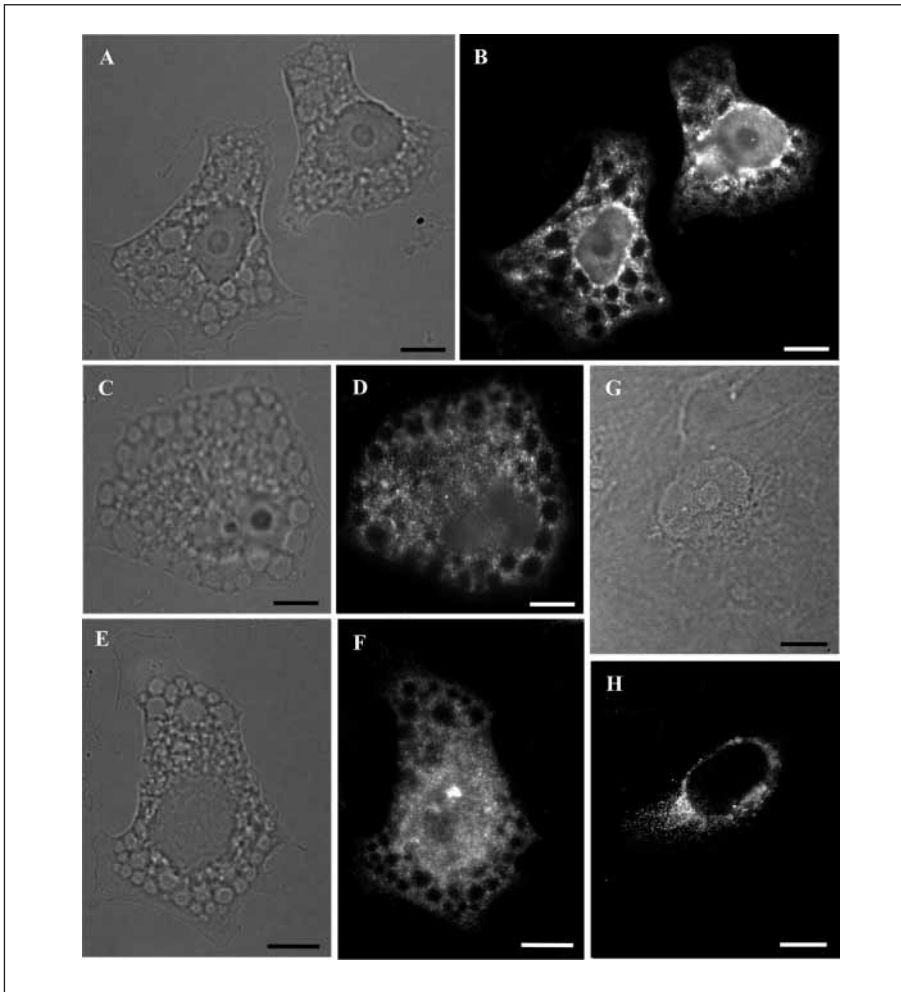


Figure 7: Immunofluorescence localisation of anti-LAMP1 antibody in HBMECs. A-F) HBMECs were treated for 24 h by VD_{90} of EHEC-Vac and stained with lysosome-specific anti-LAMP1 antibody, Alexa 488-conjugated goat anti-rabbit IgG and DAPI. A, C, and E), bright field photomicrographs; and (B, D, and F), merges of photomicrographs from Alexa 488 and DAPI channels. Anti-LAMP1 antibody localised to vacuolar membranes in EHEC-Vac-treated cells. G and H) Control (untreated) HBMECs grown for 24 h in culture medium and stained the same way display normal subcellular distribution of lysosomes. Bars represent 10 μ m. Typical results of staining with anti-LAMP1 antibody from two independent experiments are shown.

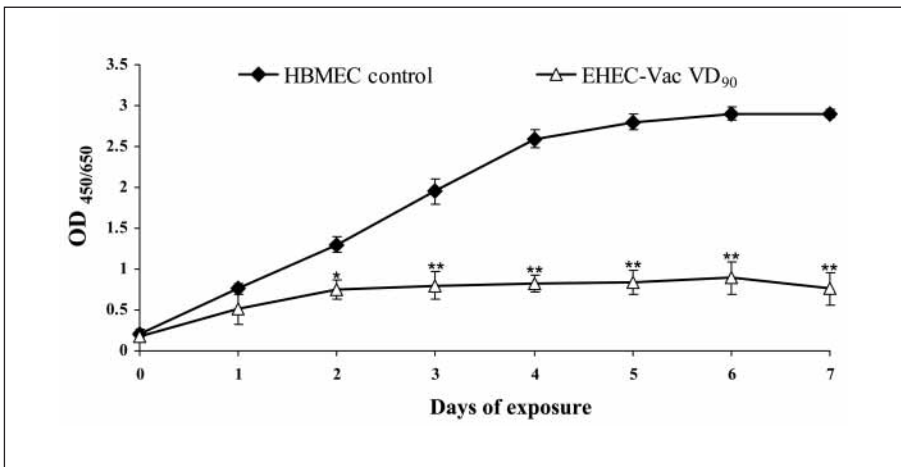


Figure 8: WST-1 assay of EHEC-Vac-treated cells. Semiconfluent HBMEC monolayers were exposed to VD_{90} of EHEC-Vac for 7 days; every day, metabolic activity was quantified spectrophotometrically ($OD_{450/650}$) using the WST-1 assay and compared to that of untreated cells. Data represent means \pm SD of three independent experiments carried out in duplicates. * $p = 0.05$, and ** $p < 0.01$ for the differences in metabolic activities of EHEC-Vac-treated vs. control cells (paired Student's *t*-test).

er time period (25.4 h). This experiment clearly demonstrated that the vacuolated cells undergo necrosis. However, probably due to the heterogeneity of unsynchronised HBMEC population, the time intervals between full vacuolisation and necrosis differ among cells in the monolayer, resulting in a stepwise, rather than a sudden, necrotic death of the population. Next to the single cell analysis data such a process is also indicated by the fact that on

day 7 after EHEC-Vac exposure a subset of vacuolated cells still survived as demonstrated by their ability to exclude trypan blue and by residual metabolic activity in the WST-1 assay (Fig. 8).

Cytokine release from HBMECs induced by EHEC-Vac

To investigate whether EHEC-Vac stimulates inflammatory response in HBMECs, release of IL-6 and IL-8 from the cells was

quantified after 24 h and 4 days of exposure to VD_{90} of EHEC-Vac. The net release of IL-6 induced by EHEC-Vac after 24 h and 4 days was 610.4 ± 9.67 pg/ml and 318.2 ± 2.15 pg/ml (mean \pm SD, three repeats), respectively. In contrast, culture supernatant of *E. coli* XL1-Blue MR strain which does not produce EHEC-Vac released <10 pg/ml of IL-6 in each time interval tested. No IL-8 response was elicited from HBMECs by VD_{90} of EHEC-Vac at any of the time points (data not shown).

Nature of EHEC-Vac

The vacuolating titer of supernatant 6451/98 was decreased two-fold and eight-fold by heating to 56°C and 70°C for 30 min, respectively. The vacuolating activity was completely destroyed by heating to 99°C for 10 min. Proteinase K (50 $\mu\text{g/ml}$) treatment (10 and 30 min) reduced the vacuolating titer from 1:16 to 1:2 and to $<1:2$, respectively, confirming its protein nature. Because vacuolating toxins produced by extraintestinal *E. coli* strains including Vat (vacuolating autotransporter toxin) (41) and Sat (secreted autotransporter toxin) (42) belong to the serine protease autotransporter family of *Enterobacteriaceae* (SPATE) (32, 33), we investigated whether or not EHEC-Vac is a serine protease. Pre-incubation of supernatant 6451/98 with the serine protease inhibitor PMSF (1 mM and 10 mM) did not reduce the vacuolating titer, though the higher concentration of PMSF was slightly toxic to the cells. This indicates that EHEC-Vac is not a serine protease.

Attempts to identify the gene(s) encoding EHEC-Vac

To identify the gene(s) encoding EHEC-Vac, we performed Southern blot hybridisation of genomic DNA from strain 6451/98 with probes derived from autotransporters with known vacuolating activity including *vacA*, *Vat* and *Sat* (Table 1). No hybridisation was observed with the *vacA* probe, nor with the *vat*, *sat-4* and *sat-6* probes which are derived from the autotransporter passenger domains that show low homology among the members of the SPATE family (32, 33). The *sat-8* probe derived from the C terminus of the autotransporter molecule which is highly conserved among SPATEs (32, 33) hybridised to a ca. 10 kb DNA fragment of strain 6451/98 (data not shown). However, nucleotide sequencing of the *sat-8* probe demonstrated 99% homology to *espP* of strain EDL933 (GenBank accession number NC_007414) indicating that the target for the probe was the *espP_E* gene present in strain 6451/98 (unpublished data).

To identify EHEC-Vac based on its morphological effects, we screened cosmids from the genomic library of strain 6451/98 for their vacuolating effect on HBMECs. However, none of 2,688 cosmids produced any apparent vacuolisation.

Endothelium-vacuolating capacity of other EHEC

None of 60 EHEC strains belonging to serotypes associated with HUS caused vacuolisation of HBMECs after 24 h and 48 h of exposure to sterile bacterial supernatants.

Discussion

The ability to cause vacuolisation in various mammalian primary cells and cell lines is one of multiple biological effects of *H. pylori* VacA which is the prototype vacuolating toxin (18, 39).

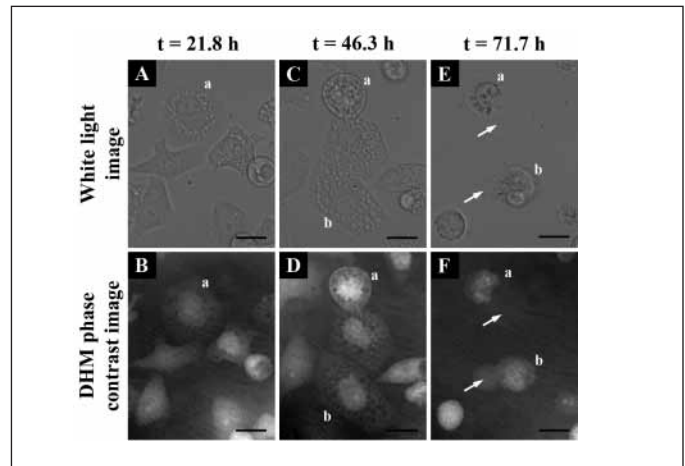


Figure 9: Necrosis of vacuolated HBMECs demonstrated using a single cell analysis. A, C, and E) white light photomicrographs of HBMECs at different time points after exposure to VD_{90} of EHEC-Vac; and (B, D, and F) corresponding quantitative digital holographic microscopy (DHM) phase contrast images. High density cell components such as the nuclei and nucleoli are visible as bright spots in the DHM phase contrast, whereas the vacuoles appear as dark areas; this indicates a low refractive index of vacuoles near or equal to that of the cell culture medium and can be interpreted as a high water content. Cells designated "a" and "b" are examples of heavily vacuolated cells which undergo necrosis after different times of exposure to EHEC-Vac (49.9 h and 25.4 h, respectively). Arrows in panels E and F indicate liberation of the cytoplasmic content from the necrotic cells. The white light and DHM quantitative phase contrast images shown are representatives of behaviour of 25 cells investigated.

However, toxins with similar phenotypic effects have also been identified in other bacterial species and include mainly autotransporters (32, 33, 41, 42) and pore-forming toxins (25, 26, 43–45). Examples of the first group are, besides *VacA*, *Vat* produced by avian pathogenic *E. coli* (41) and UPEC strains (unpublished data) and *Sat* recently identified in UPEC strain CFT073 (33, 42). Pore-forming toxins with vacuolating activity are haemolysins of *Vibrio cholerae* (25, 26, 43) and *Serratia marcescens* (44) and aerolysin of *Aeromonas hydrophila* (45). Recently, vacuolating activity has also been reported for the subtilase cytotoxin produced by an EHEC strain (46) (Table 2). The EHEC-Vac identified in this study based on its biological activity extends the spectrum of vacuolating toxins and is, to our knowledge, the first vacuolating toxin acting on endothelial cells.

EHEC-Vac-induced vacuoles resemble most closely those produced by *VacA* (Table 2). Specifically, both types of vacuoles stain with neutral red indicating their acidic microenvironment. This is consistent with the origin of vacuoles induced by both organisms from the late endocytic compartments (late endosomes/lysosomes in *H. pylori* [47, 48] and lysosomes in EHEC) (Table 2). Moreover, the mechanism of vacuolisation caused by *H. pylori* *VacA* involves formation of anion-selective channels in the membranes of late endocytic compartments (38) resulting in an increased intraluminal chloride concentration. To compensate for the increased anion concentration, vacuolar ATPase activity increases, increasing proton pumping into the vacuole that reduces vacuolar pH (39). Because of the central role of the vacuo-

Table 2: Comparison of vacuoles induced by EHEC-Vac with those caused by other vacuolating toxins.

Toxin (Species)	Examples of vacuolated cells	Origin of vacuoles (cell line)	Staining with neutral red	Effect of bafilomycin A1 on the toxin-induced vacuolisation	Reference
EHEC-Vac (<i>E. coli</i>) EHEC	HBMEC GMVEC	lysosomes	yes	Inhibits vacuole formation Reverts vacuolisation (=causes disappearance of preformed vacuoles)	This study
VacA (<i>H. pylori</i>)	Intestine 407, HeLa, Hep-2, Vero, BHK, etc.	Late endosomes/ lysosomes (HeLa, BHK)	yes	Inhibits vacuole formation Reverts vacuolisation	24, 37, 47, 48
Haemolysin (<i>V. cholerae</i>)	Vero HeLa	Early vacuoles (1–4 h) – ER Late vacuoles (16 h) – autophagosomes (Vero)	Early vacuoles – subset Late vacuoles – all	Does not inhibit vacuole formation Exacerbates vacuolisation	25, 26, 43
Haemolysin (<i>S. marcescens</i>)	HeLa HEp-2	NI	no	Neither inhibits nor reverts vacuolisation	44
Aerolysin (<i>A. hydrophila</i>)	BHK CHO MDCK	ER (BHK)	NI	NI	45
Vat (<i>E. coli</i>) APEC, ExPEC	CEF PCK	NI	yes	NI	41
Sat (<i>E. coli</i>) ExPEC	CRL-1749 CRL-1573	NI	NI	NI	42
Subtilase cytotoxin (<i>E. coli</i>) EHEC	Vero	NI	Yes	Inhibits vacuole formation	46

EHEC-Vac, enterohemorrhagic *E. coli* vacuolating cytotoxin; VacA, vacuolating cytotoxin; Vat, vacuolating autotransporter toxin; Sat, secreted autotransporter toxin; APEC, avian pathogenic *E. coli*; ExPEC, extra-intestinal *E. coli*; HBMEC, human brain microvascular endothelial cells; GMVEC, human glomerular microvascular endothelial cells; BHK, baby hamster kidney; CHO, Chinese hamster ovary; MDCK, Madin-Darby canine kidney; CEF, chicken embryonal fibroblasts; PCK, primary chicken kidney; CRL-1749, human bladder epithelial cells; CRL-1573, human kidney epithelial cells; ER, endoplasmic reticulum; NI, not investigated.

lar proton pump in the vacuole formation, specific inhibitors of the vacuolar-type H⁺-ATPase such as bafilomycin A1 effectively counteract the vacuolisation caused by VacA (24, 37). The fact that bafilomycin A1 both prevented and reverted vacuolisation mediated by EHEC-Vac suggests that the mechanism of vacuole formation by EHEC-Vac might also involve the vacuolar-type ATPase activation. This characteristic, which EHEC-Vac shares with VacA and also with the subtilase cytotoxin (Table 2), differentiates this toxin from other vacuolating toxins which have been studied in this respect, specifically from haemolysins of *V. cholerae* and *S. marcescens* (Table 2). These toxins induce vacuolisation which is not inhibited but is rather exacerbated by bafilomycin A1 and other inhibitors of the vacuolar proton pump (25, 26, 44). Notably, the vacuoles induced by these toxins have a different origin than those induced by VacA and EHEC-Vac, arising from endoplasmic reticulum (26).

Despite its striking similarity to VacA in its phenotype and the character of the vacuoles it produces, EHEC-Vac is apparently a protein unrelated (or only distantly related) to VacA at the genomic level as indicated by the failure of the genomic DNA of strain 6451/98 to hybridise with a *vacA* probe. Moreover, based on the Southern blot hybridisation, EHEC-Vac is also distinct from two other vacuolating toxins, specifically Vat (41) and Sat

(33, 42), produced by extraintestinal *E. coli* strains. Finally, EHEC-Vac of strain 6451/98 is distinct from the subtilase cytotoxin because this strain lacks the *subA/subB* genes, and it is not a haemolysin since the strain is non-haemolytic on both blood agar and enterohaemolysin agar. We were also unable to identify the gene encoding the protein responsible for the vacuolating activity of strain 6451/98 by analysing 2,688 cosmids from the genomic library of this strain for vacuolating activity towards HBMECs, because none of the cosmids displayed a clear vacuolating phenotype. This suggests that a multi-component system, from which not all components are present in a cosmid, might be required for the expression of this phenotype, as has been shown for the expression of attaching-effacing lesions induced by EHEC (49). Regardless of its precise identity which is presently under investigation, our data suggest that EHEC-Vac might contribute to the virulence of EHEC, similarly as demonstrated or hypothesised for other vacuolating toxins including VacA (39), Sat in UPEC (42), Vat in avian pathogenic *E. coli* (41), and aerolysin in *A. hydrophila* (50). The cytopathic effect of EHEC-Vac on human microvascular endothelial cells including extensive vacuolisation followed by necrosis identifies this molecule as a putative virulence factor that might contribute to the microvascular injury underlying HUS. Moreover, the ability of EHEC-

Vac to elicit IL-6 release from microvascular endothelial cells represents an additional mechanism by which the toxin might contribute to the pathogenesis of HUS, in particular in its early phase (2, 6).

The absence of EHEC-Vac in EHEC of the major serotypes associated with HUS does not preclude contribution of this toxin to the pathogenesis of HUS. Recent findings of various non-Stx virulence factors including toxins and adhesins in EHEC associated with HUS (6, 14, 16, 17) indicate that HUS is a multifactorial consequence of EHEC infection, that involves a cocktail of virulence determinants that synergistically cause profound vascular injury (6). Notably, not all components of this cocktail are produced by all EHEC associated with HUS, but the virulence profiles are rather serotype-specific (1, 12). Accordingly, though EHEC-Vac is dispensable for endothelial injury caused by EHEC O157 and the major non-O157 HUS-associated EHEC which produce other endothelium-injuring toxins, such as Stx, EHEC haemolysin or CDT-V (14, 16), it may be essential for

virulence of strain 6451/98 which lacks these determinants. Similar to CDT-V (12), production of EHEC-Vac is apparently restricted only to particular EHEC serotypes.

Vacuolisation of the host cells is yet incompletely understood mechanism in the EHEC pathogenesis, but its significance is supported, besides our study, by finding of vacuolated intestinal epithelial cells in monkeys experimentally infected with EHEC O157:H7 (51). Further studies should identify additional human cell types sensitive to EHEC-Vac and to clarify the role of this toxin in the pathogenesis of EHEC-mediated diseases.

Acknowledgements

We thank Dr. Phillip I. Tarr (Washington University School of Medicine, St. Louis, Mo., USA) for critical reading of the manuscript and helpful comments. The excellent technical assistance of Margret Junge (Institute for Hygiene, Münster), Angelika Vollmer and Steffi Ketelhut (Center for Biomedical Optics and Photonics, Münster), and Barbara Plaschke (Institute for Molecular Infection Biology, Würzburg) is highly appreciated.

References

- Karch H, Tarr PI, Bielaszewska M. Enterohaemorrhagic *Escherichia coli* in human medicine. *Int J Med Microbiol* 2005; 295: 405–418.
- Tarr PI, Gordon CA, Chandler WL. Shiga-toxin-producing *Escherichia coli* and haemolytic uraemic syndrome. *Lancet* 2005; 365: 1073–1086.
- Andreoli SP, Trachtman H, Acheson DWK, et al. Hemolytic uraemic syndrome: epidemiology, pathophysiology, and therapy. *Pediatr Nephrol* 2002; 17: 293–298.
- Richardson SE, Karmali MA, Becker LE, et al. The histopathology of the hemolytic uraemic syndrome associated with verocytotoxin-producing *Escherichia coli* infections. *Hum Pathol* 1988; 19: 1102–1108.
- Upadhyaya K, Barwick K, Fishaut M, et al. The importance of nonrenal involvement in hemolytic-uraemic syndrome. *Pediatrics* 1980; 65: 115–120.
- Bielaszewska M, Karch H. Consequences of enterohaemorrhagic *Escherichia coli* infection for the vascular endothelium. *Thromb Haemost* 2005; 94: 312–318.
- Dehio C. Bartonella interactions with endothelial cells and erythrocytes. *Trends Microbiol* 2001; 9: 279–285.
- Sandvig K. Shiga toxins. *Toxicon* 2001; 39: 1629–1635.
- Müthing J, Schweppe CH, Karch H, et al. Shiga toxins, glycosphingolipid diversity, and endothelial cell injury. *Thromb Haemost* 2009; 101: 252–264.
- Janka A, Bielaszewska M, Dobrindt U, et al. Cytotolethal distending toxin gene cluster in enterohaemorrhagic *Escherichia coli* O157:H⁻ and O157:H7: characterization and evolutionary considerations. *Infect Immun* 2003; 71: 3634–3638.
- Friedrich AW, Lu S, Bielaszewska M, et al. Cytotolethal distending toxin in *Escherichia coli* O157:H7: spectrum of conservation, structure, and endothelial toxicity. *J Clin Microbiol* 2006; 44: 1844–1846.
- Bielaszewska M, Fell M, Greune L, et al. Characterization of cytotolethal distending toxin genes and expression in Shiga toxin-producing *Escherichia coli* strains of non-O157 serogroups. *Infect Immun* 2004; 72: 1812–1816.
- Schmidt H, Beutin L, Karch H. Molecular analysis of the plasmid-encoded hemolysin of *Escherichia coli* O157:H7 strain EDL 933. *Infect Immun* 1995; 63: 1055–1061.
- Bielaszewska M, Sinha B, Kuczius T, et al. Cytotolethal distending toxin from Shiga toxin-producing *Escherichia coli* O157 causes irreversible G2/M arrest, inhibition of proliferation and death of human endothelial cells. *Infect Immun* 2005; 73: 552–562.
- Schmidt H, Maier E, Karch H, et al. Pore-forming properties of the plasmid-encoded hemolysin of enterohaemorrhagic *Escherichia coli* O157:H7. *Eur J Biochem* 1996; 241: 594–601.
- Aldick T, Bielaszewska M, Zhang W, et al. Hemolysin from Shiga toxin-negative *Escherichia coli* O26 strains injures microvascular endothelium. *Microbes Infect* 2007; 9: 282–290.
- Paton AW, Srimanote P, Talbot UM, et al. A new family of potent AB₅ cytotoxins produced by Shiga-toxic *Escherichia coli*. *J Exp Med* 2004; 200: 35–46.
- Leunk RD, Johnson PT, David BC, et al. Cytotoxic activity in broth-culture filtrates of *Campylobacter pylori*. *J Med Microbiol* 1988; 26: 93–99.
- Zhang W, Bielaszewska M, Friedrich AW, et al. Transcriptional analysis of genes encoding Shiga toxin 2 and its variants in *Escherichia coli*. *Appl Environ Microbiol* 2005; 71: 558–561.
- Brzuszkiewicz E, Bruggemann H, Liesegang H, et al. How to become a uropathogen: Comparative genomic analysis of extraintestinal pathogenic *Escherichia coli* strains. *Proc Natl Acad Sci USA* 2006; 103: 12879–12884.
- Welch RA, Burland V, Plunkett G. III, et al. Extensive mosaic structure revealed by the complete genome sequence of uropathogenic *Escherichia coli*. *Proc Natl Acad Sci USA* 2002; 99: 17020–17024.
- Stins MF, Gilles F, Kim KS. Selective expression of adhesion molecules on human brain microvascular endothelial cells. *J Neuroimmunol* 1997; 76: 81–90.
- van Setten PA, van Hinsbergh VWM, van der Velden TJAN, et al. Effects of TNF on verocytotoxin cytotoxicity in purified human glomerular microvascular endothelial cells. *Kidney Int* 1997; 51: 1245–1256.
- Cover TL, Reddy LY, Blaser MJ. Effects of ATPase inhibitors on the response of HeLa cells to *Helicobacter pylori* vacuolating toxin. *Infect Immun* 1993; 61: 1427–1431.
- Coelho A, Andrade JR, Vicente AC, et al. Cytotoxic cell vacuolating activity from *Vibrio cholerae* hemolysin. *Infect Immun* 2000; 68: 1700–1705.
- Figuroa-Arredondo P, Heuser JE, Akopyants NS, et al. Cell vacuolation caused by *Vibrio cholerae* hemolysin. *Infect Immun* 2001; 69: 1613–1624.
- Kügler S, Böcker K, Heusipp G, et al. Pertussis toxin transiently affects barrier integrity, organelle organization and transmigration of monocytes in a human brain microvascular endothelial cell barrier model. *Cell Microbiol* 2007; 9: 619–632.
- Nicoletti I, Migliorati G, Pagliacci MC, et al. A rapid and simple method for measuring thymocyte apoptosis by propidium iodide and flow cytometry. *J Immunol Methods* 1991; 139: 271–279.
- Kemper B, Carl D, Höink A, et al. Modular digital holographic microscopy system for marker-free quantitative phase contrast imaging of living cells. *Proc SPIE* 2006; 6191: 61910T.1–61910T.8.
- Kemper B, Carl D, Schnekenburger J, et al. Investigation of living pancreas tumor cells by digital holographic microscopy. *J Biomed Opt* 2006; 11: 34005.
- Tomb JF, White O, Kerlavage AR, et al. The complete genome sequence of the gastric pathogen *Helicobacter pylori*. *Nature* 1997; 388: 539–547.
- Parreira VR, Gyles CL. A novel pathogenicity island integrated adjacent to the thrW tRNA gene of avian pathogenic *Escherichia coli* encodes a vacuolating autotransporter toxin. *Infect Immun* 2003; 71: 5087–5096.
- Guyer DM, Henderson IR, Nataro JP, et al. Identification of Sat, an autotransporter toxin produced by uropathogenic *Escherichia coli*. *Mol Microbiol* 2000; 38: 53–66.
- Ewers C, Janssen T, Kiessling S, et al. Molecular epidemiology of avian pathogenic *Escherichia coli* (APEC) isolated from colisepticemia in poultry. *Vet Microbiol* 2004; 104: 91–101.
- Cover TL, Puryear W, Perez-Perez GI, et al. Effect of urease on HeLa cell vacuolation induced by *Helicobacter pylori* cytotoxin. *Infect Immun* 1991; 59: 1264–70.
- Bowman EJ, Siebers A, Altendorf K. Bafilomycins: a class of inhibitors of membrane ATPases from micro-

- organisms, animal cells, and plant cells. *Proc Natl Acad Sci USA* 1988; 85: 7972–7976.
37. Papini E, Bugnoli M, De Bernard M, et al. Bafilomycin A1 inhibits *Helicobacter pylori*-induced vacuolization of HeLa cells. *Mol Microbiol* 1993;7: 323–327.
38. Szabò I, Brutsche S, Tombola F, et al. Formation of anion-selective channels in the cell plasma membrane by the toxin VacA of *Helicobacter pylori* is required for its biological activity. *EMBO J* 1999;18: 5517–5527.
39. Cover TL, Blanke SR. *Helicobacter pylori* VacA, a paradigm for toxin multifunctionality. *Nat Rev Microbiol* 2005; 3: 320–332.
40. Holtzman E. Lysosomes. Springer Verlag, 2007.
41. Salvadori MR, Yano T, Carvalho HE, et al. Vacuolating cytotoxin produced by avian pathogenic *Escherichia coli*. *Avian Dis.* 2001; 45: 43–51.
42. Guyer DM, Radulovic S, Jones FE, et al. Sat, the secreted autotransporter toxin of uropathogenic *Escherichia coli*, is a vacuolating cytotoxin for bladder and kidney epithelial cells. *Infect Immun* 2002; 70: 4539–4546.
43. Mitra R, Figueroa P, Mukhopadhyay AK, et al. Cell vacuolation a manifestation of the El Tor hemolysin of *Vibrio cholerae*. *Infect. Immun* 2000; 68: 1928–1933.
44. Hertle R, Hilger M, Weingardt-Kocher S, et al. Cytotoxic action of *Serratia marcescens* hemolysin on human epithelial cells. *Infect Immun* 1999; 67: 817–825.
45. Abrami L, Fivaz M, Glauser PE, et al. A pore-forming toxin interacts with a GPI-anchored protein and causes vacuolation of the endoplasmic reticulum. *J Cell Biol* 1998; 140: 525–540.
46. Morinaga N, Yahiro K, Matsuura G, et al. Two distinct cytotoxic activities of subtilase cytotoxin produced by shiga-toxigenic *Escherichia coli*. *Infect Immun* 2007; 75: 488–496.
47. Papini E, de Bernard M, Milia E, et al. Cellular vacuoles induced by *Helicobacter pylori* originate from late endosomal compartments. *Proc Natl Acad Sci USA* 1994; 91: 9720–9724.
48. Molinari M, Galli C, Norais N, et al. Vacuoles induced by *Helicobacter pylori* toxin contain both late endosomal and lysosomal markers. *J Biol Chem* 1997; 272: 25339–25344.
49. Reading NC, Torres AG, Kendall MM, et al. A novel two-component signaling system that activates transcription of an enterohemorrhagic *Escherichia coli* effector involved in remodeling of host actin. *J Bacteriol* 2007; 189: 2468–2476.
50. Guimarães MS, Andrade JR, Freitas-Almeida AC, et al. *Aeromonas hydrophila* vacuolating activity in the Caco-2 human enterocyte cell line as a putative virulence factor. *FEMS Microbiol Lett* 2002; 207: 127–131.
51. Kang G, Pulimood AB, Koshi R, et al. A monkey model for enterohemorrhagic *Escherichia coli* infection. *J Infect Dis* 2001; 184: 206–210.